International Journal of Fluid Machinery and Systems
Vol. 11, No. 2, April-June 2018
DOI: http://dx.doi.org/10.5293/IJFMS.2018.11.2.146
ISSN (Online): 1882-9554

Original Paper

Hydrodynamic Damping of a Fluttering Hydrofoil in High-speed Flows

Carl W. Bergan[1], Bjørn W. Solemslie[1], Petter Østby[2,3] and Ole G. Dahlhaug[1]

[1]Waterpower Laboratory, Norwegian University of Science and Technology
Alfred Getz v. 4, 7034 Trondheim, Norway,
carl.w.bergan@ntnu.no, bjorn.w.solemslie@ntnu.no, ole.g.dahlhaug@ntnu.no
[2]Department of Mechanical and Industrial Engineering Norwegian University of Science and Technology
Richard Birkelands vei 2B, 7034 Trondheim, Norway
[3]Rainpower AS Instituttveien 8, 2027 Kjeller, Norway, petter.oestby@rainpower.no

Abstract

A hydrofoil resembling a high head Francis runner blade was submerged in a rectangular channel and attached to the walls in a fixed-beam configuration. The hydrofoil was excited by piezoelectric Macrofiber composite actuators (MFCs), and the vibration was measured at the trailing edge with Laser Doppler Vibrometry (LDV) and semiconductor strain gauges. The hydrofoil was exposed to water velocities ranging from 0 to 25 m/s. Lock-in occurred at approx. 11 m/s. The damping increased linearly with the water velocity, with a slope of 0.02 %/(m/s) below lock-in, and 0.13 %/(m/s) above lock-in. The natural frequency of the foil increased slightly with increasing water velocity below lock-in, due to the added stiffness of the passing water. Additionally, the natural frequency increased significantly when passing through lock-in, due to the vortex shedding phase shift.

Keywords: FSI, Damping, Francis, FRF

1. Introduction

In the current energy market, there is a push towards higher power concentration in turbines, causing them to be more susceptible to problems caused by Fluid Structure Interactions (FSI), such as fatigue cracking, vibration and resonance [1, 2]. Pressure pulsations and vibrations can cause devastating structural damage, due to the high number of cycles a turbine blade can experience within a day [3]. The key to prevent this, is to be able to predict a runner's dynamic properties in the design phase.

The dynamic response of a Francis runner is, in addition to the hydraulic excitation, dependent on two components: the natural frequency of the runner, and the fluid damping [4]. The present work takes an experimental approach to determine the damping factor in an open reference case, to be used as validation for simulation.

The vibrational magnitudes close to resonance of any vibrating system is strongly dependent of the damp- ening factor of the system [5]. In the design of a Francis runner, it is important to predict which frequencies will cause the runner blades to resonate. It is also important to be able to predict the magnitude of vibration in these frequency domains, in order to understand how the turbine will perform if exposed to those conditions. Most of the work that has been performed on vibrating hydrofoils in flowing water has dealt with relatively low velocity ranges. The highest velocities seen in earlier measurements were 25 m/s[3], and most of the previous work is below 15 m/s. For a high head Francis runner, typical velocities are in the range of 35 to 45 m/s, so high-velocity damping measurements are of particular interest.

The damping appears to be linear with respect to velocity, from both experimental and theoretical work [3, 4, 6, 7], but the experimental uncertainty grows in the high velocity range [3]. The literature is inconclusive with respect to the effect on natural frequency. Coutu found that the natural frequency remained unchanged with respect to water velocity well above lock-in, but the large uncertainty band leaves some ambiguity in the conclusion[3]. Yao found that the natural frequency increased through the lock-in region [6]. However, the experiments performed by Yao were on a hydrofoil constrained in a cantilever fashion, which are prone to vibrational modes not strictly relevant for a Francis runner. In fact, most of the work performed with submerged hydrofoils employs a cantilever hydrofoil[7, 8, 9].

Received June 23 2017; revised September 28 2017; accepted for publication December 23 2017: Review conducted by Yoshinobu Tsujimoto. (Paper number O17043J)
Corresponding author: Carl W. Bergan, carl.w.bergan@ntnu.no

2. Materials and Methods

The tests were performed in a straight Ø300 mm pipe section available at the Waterpower Laboratory at the Norwegian University of Science and Technology (NTNU). The length of the pipeline is approx. 28 m, and the test section was placed close to the middle of this stretch. The test section is shown in Fig. 1.

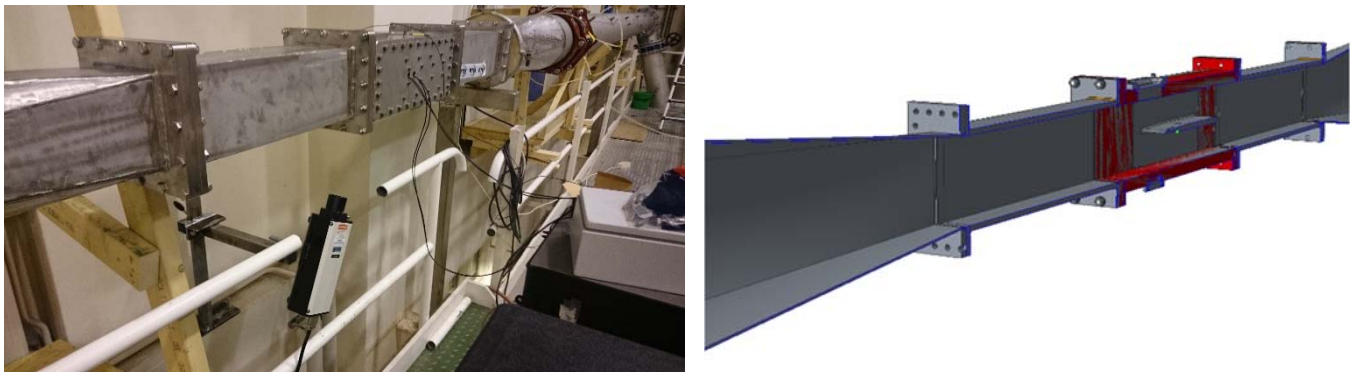

(a)Picture of test rig (b) Sliced CAD model of test rig

Fig. 1 Test section placed in the straight pipeline. The 300 mm circular cross section is changed to a 150x150 mm2 rectangular cross section.

The test section was designed to ensure a sufficient stiffness, in order to provide a grounded support for the test structure, i.e. the hydrofoil, as is good practice for modal testing [10]. This also enables the assumption of stiff walls for boundary conditions when performing structural simulations.

The hydrofoil geometry was long and slender, with a thickness of 12 mm and a cord length of 250 mm. After 150 mm, the thickness was tapered down to 4.5 mm at the trailing edge, before being chamfered and rounded on one side, as is normal for runner blades. The hydrofoil was milled from a single piece of aluminium alloy, and grooves were milled for instrumentation and cables. A cord wise cross section of the foil is shown in Fig. 2.

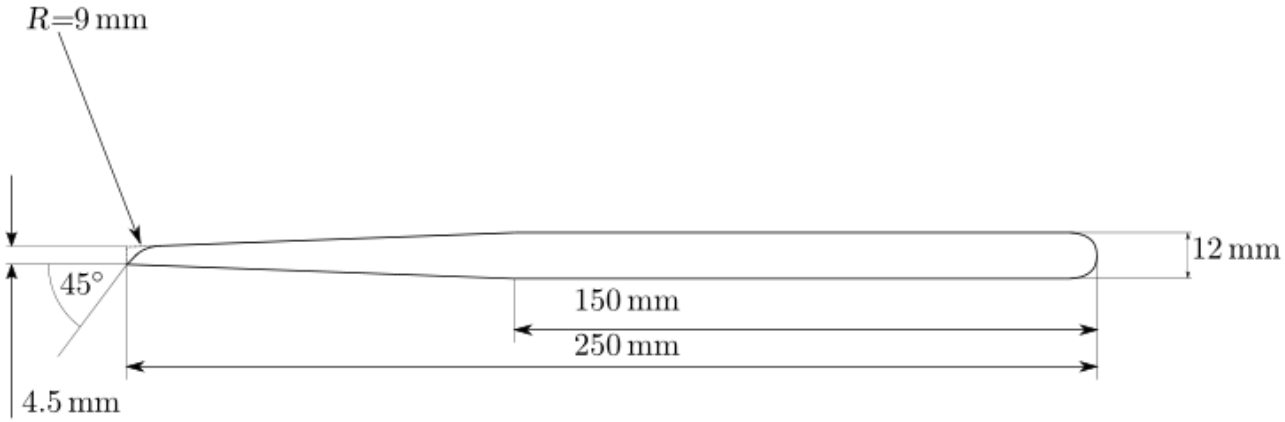

Fig. 2 2D view of the hydrofoil with dimensions

The hydrofoil was mounted without any angle of attack, and was then excited using piezoelectric Macrofiber composite (MFCs) actuators from PI Ceramic. Two MFCs were mounted on each side of the foil at the width wise center, close to the trailing edge. By exciting these in a sinusoidal pattern phase-separated by 180◦, a bending action is induced in the blade. A schematic of this type of excitation can be seen in Fig. 3.

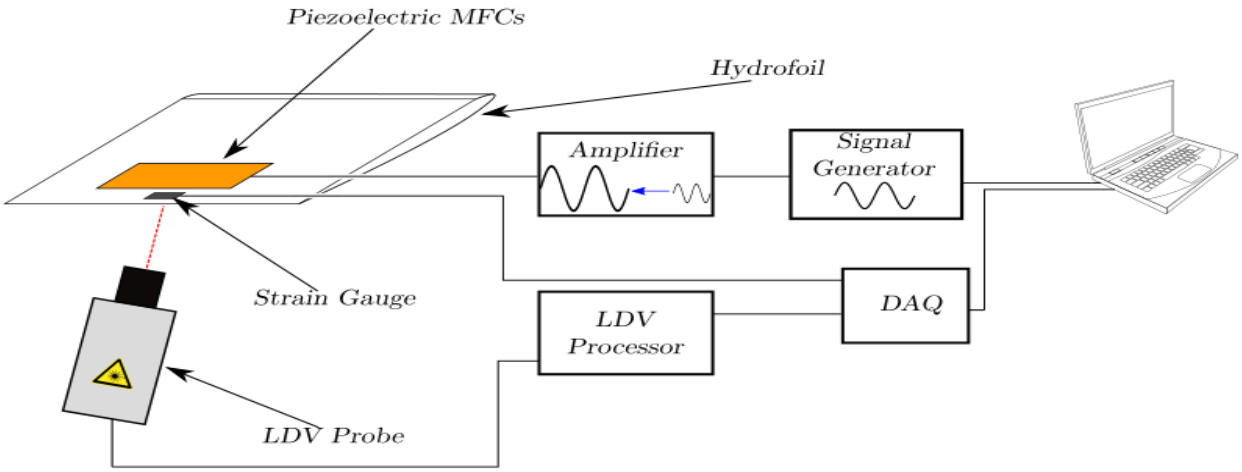

Fig. 3 Schematic of the experimental setup

In order to measure the vibrational amplitude, semiconductor strain gauges from Kulite were mounted on the trailing edge of the hydrofoil, directly downstream the MFCs.

In addition to strain gauges, the vibrational amplitude was measured using Laser Doppler Vibrometry (LDV) equipment from Polytech. LDV is a non-intrusive measurement method that measures vibration using the Doppler-shifted reflection of laser light. The LDV measures vibration in a single spot, along the axis of the laser beam, and the measurement point was located at the trailing edge of the foil.

The tests were performed using a Stepped-Sine excitation, in which a series of constant-frequency excitations are performed in order to avoid transient effects when moving through a resonant region [10].

Each measurement consisted of approx. 60 excited frequencies, and each measurement was repeated 30 times in order to obtain sufficient statistics for an assessment the uncertainty in both damping and natural frequency. The tests were performed with water speeds ranging from 0 to 25 m/s, with steps of 5 m/s. The test rig was pressurized in order to obtain cavitation-free conditions.

3. Results and Discussion

The experiments were successfully conducted with water velocities up to 25 m/s, without cavitation. Frequency analysis using the Welch method, as implemented by MATLAB, was conducted on the excitation signal and on the response of the hydrofoil, in order to generate a frequency response curve around the measured mode. The Welch method is an estimate of the power spectrum, which reduces the power noise by reducing the frequency resolution through averaging. For this experiment, such a trade-off was deemed appropriate, as the damping estimate is sensitive to the estimated amplitudes.

The damping was estimated using the Circle-Fit Method, also known as the Kennedy-Pancu Method. The method yields the damping ratio through a geometric investigation in the complex plane. By plotting the real and imaginary parts of the frequency response data in the complex plane, a resonant peak will appear as a circle, as shown in Fig. 4. It can then be shown that the damping ratio can be calculated through the following geometric relations:

$$\zeta = \frac{\omega_b - \omega_a}{\omega_a \tan(\theta_a/2) + \omega_b \tan(\theta_b/2)} \tag{1}$$

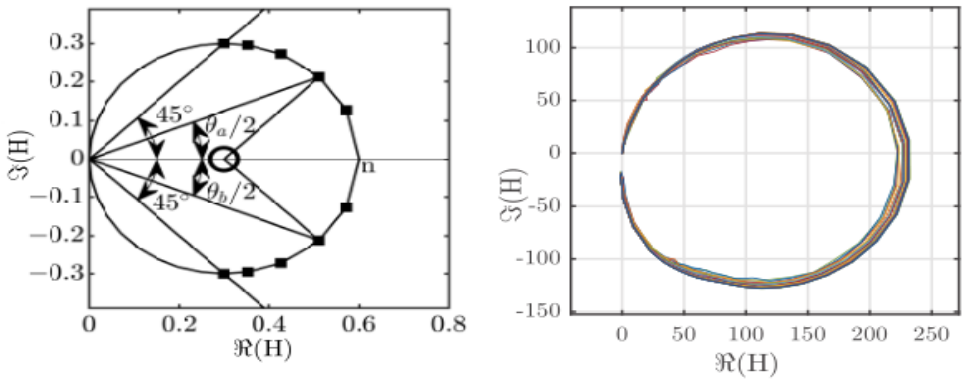

(a)Circle fit (b) Nyquist plot

Fig. 4 Nyquist plot of ideal and real data. In this plot, H is the complex frequency response of the vibrating system

In eq. (1), ωa and ωb denote the frequency at points a and b respectively, and ζ is the damping. The Circle-Fit Method is described in more detail by Craig and Kurdila in Fundamentals of structural dynamics[5]. By repeating the above measurement several times, the uncertainty in the modal parameters can be esti-mated with the student-t distribution.

3.1 Damping and natural frequency

The resulting damping ratios and natural frequencies are shown in Fig. 5.

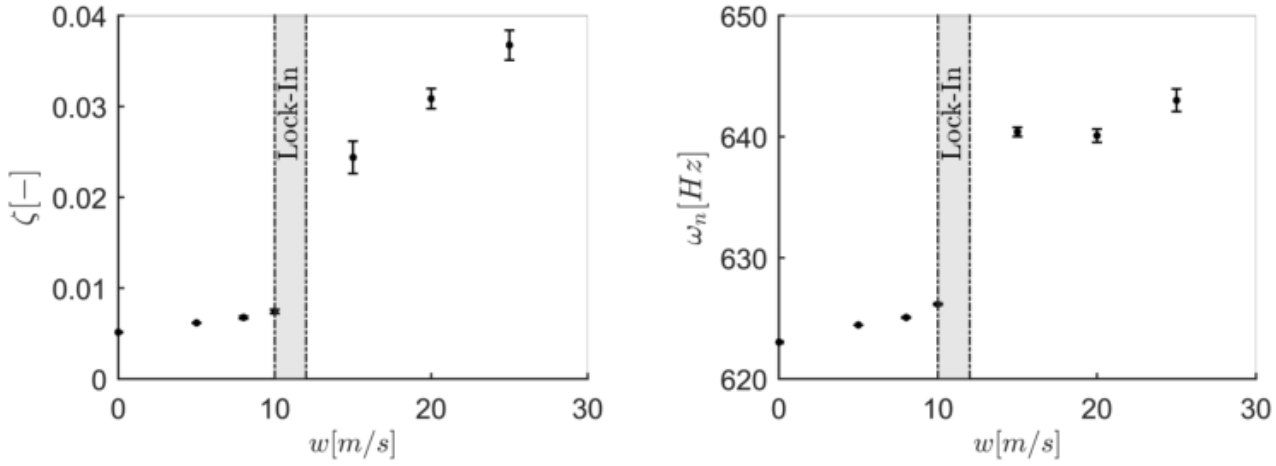

(a)Damping ratio (b) Natural frequency

Fig. 5 Damping and natural frequency

As indicated by Fig. 5(a), there is a clear correlation between the water velocity, and the damping factor of the vibrating system. Furthermore, this correlation seems to undergo some change around 10 to 12 m/s. In fact, this is the velocity where the frequency of the vortex shedding resonates with the natural frequency of the hydrofoil, commonly referred to as ”lock-in”. This change around lock-in was previously observed, for the torsional vibration mode of a cantilever beam [6]. It should be noted that the torsional mode of the cantilever beam is similar to the second bending mode of a fixed beam, and it is expected that the dynamic behavior of the two modes are similar. Although the present work has not investigated the second bending mode, it is thought to behave similarly to the first bending mode. In the vicinity of lock-in, the natural frequency of the foil undergoes an abrupt change, from 625 Hz to 640 Hz. There is no apparent trend above lock-in, and it may.

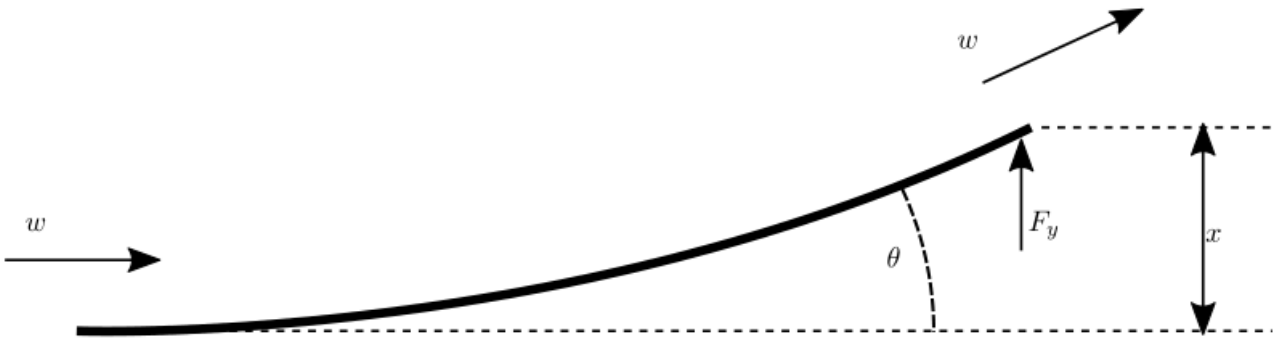

Fig. 6 Force balance on a bent beam.

The water approaching from the left is being deflected by the beam, shown as a thick black line. This in turn exerts a force on the beam, which is proportional to the deflection and to the water velocity squared very well be that the natural frequency is constant in that region. This corresponds with previous findings [3], where the natural frequency was found to be independent of the water velocity.

For velocities well below lock-in, there is a clear linear increase in the natural frequency of the foil. This increasing trend in dampened natural frequency conforms with what may be modeled as a spring with increasing stiffness, due to the water being deflected over the hydrofoil. If we consider a bent plate deflecting water, as shown in Fig. 6, the force on the plate from the water being deflected would be proportional to the deflection according to eq. (2). This is indeed the case in the present measurements, since the deflection was measured at the trailing edge, and the water will therefore also be deflected.

$$F_y \propto w^2 \cdot \sin(\theta) \tag{2}$$

In eq. (2), the proportionality between the force and the velocity will account for a stiffening spring as the water velocity is increased, indicating a higher natural frequency.

Fy $\propto$ sin (θ) will be equivalent to Fy $\propto$ θ for small values of θ, meaning for small deflections at the trailing edge. By considering the geometric deformation of the trailing edge, it is evident that the angle at the trailing edge is proportional to the deflection through the relation shown in eq. (3).

$$\theta \propto \arctan(x) \tag{3}$$

Equation 3 will be equivalent to θ $\propto$ x for small deflections. Hence the force exerted on the blade by the deflected water should be proportional to the deflection and the water velocity squared.

The stiffness of the spring will increase as the water velocity increases, effectively increasing the spring constant acting on the vibrating system. It can be argued that such an increase in stiffness will account for the observed increase in natural frequency. The scale of this effect is, however, rather small, and is quickly dominated by other effects as the damping increases. This could indicate that the effect is only significant below lock-in, as indicated by Fig. 5(b). A more thorough theoretical investigation of the forces working on the hydrofoil above lock-in can be found in [4], where the added stiffness is assumed to be negligible.

3.2 Vortex shedding resonance

During the experiments, the vortex shedding reached resonance with the hydrofoil. The resonance occurred at approx. 11 m/s, which correspond well with the theoretical Von Karman frequency, as described in subsection 3.3. This resonance is particularly problematic, as it is on the same order of magnitude as the excitation amplitude. As such, there is no reliable data available in the range 10 to 12 m/s. In order to quantify the effect from lock-in, a vibration study was carried out without excitation from the MFC patches. Fig. 7 shows the level of vibration across the frequency spectrum both with and without excitation.

As shown in Fig. 7, there is significant excitation from the vortex shedding in the vicinity of the lock-in velocity, but the shedding excitation becomes negligible outside of the range 9 to 12 m/s. Determining the damping ratio in the lock-in region is difficult, due to the added force of the vortex shedding. However, the foil behavior close to lock-in is quite interesting both above and below lock-in.

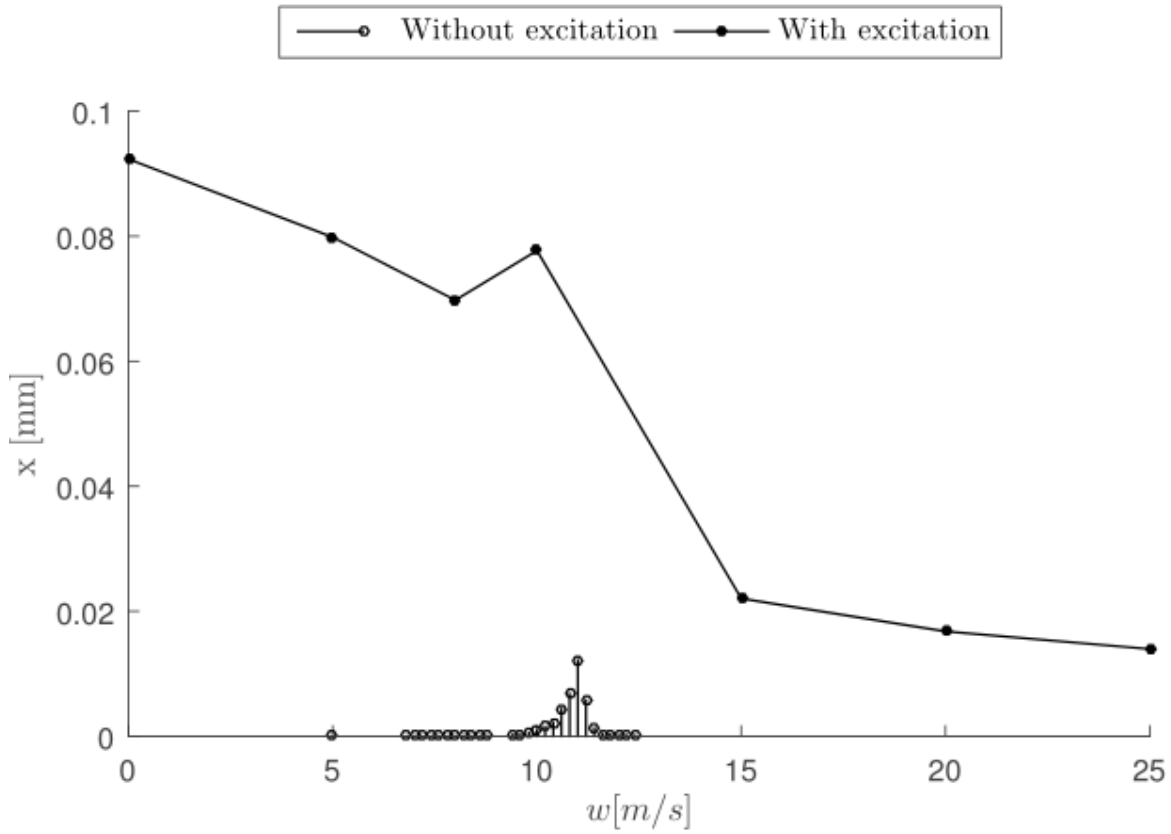

Fig. 7 Measured vibrational amplitudes with and without MFC excitation.

Looking back at Fig. 5(a), the behavior is quite different when comparing results for velocities below and above lock-in. There is a large jump in the natural frequency, and the change in damping ratio takes on a steeper slope.

3.3 Von Karman Damping

Williamson [11] showed that the phase angle between the vortex shedding and the movement of the structure changes through the locking region much like the phase change of a 1 Degree of Freedom (DOF) mass spring system changes through resonance. Using this, one can model the foil and vortex street as a 2 DOF system where eq. (4) is the foil/water system while eq. (5) expresses the vortex shedding:

$$\ddot{x} + 2\zeta\omega_n\dot{x} + \omega_n^2 x = a \cdot C_l \tag{4}$$

$$\ddot{C}_l + 2\zeta_c\omega_c\dot{C}_l + \omega_c^2 C_l = b \cdot \dot{x} \tag{5}$$

In the equations above, Cl is the lift, a and b are constants, x is the foil deflection, ωn is the natural frequency of the foil, ωc is the frequency of the vortex shedding, ζ is the damping of the foil and ζc is the damping of the vortex shedding.

These equations are a simplified version of the van der Pol type oscillator proposed by Bishop and Hassan [12]. Their model contains some non-linear terms which model the hysteresis near lock-in and self exciting phenomena. These are removed in eq. (5) as there are not any reliable measurements in the lock-in region. The eigen frequency of the foil, ωn , is known from the measurements at no velocity, w . The damping of the foil water system ζ without regards for the vortex interaction increase linearly with flow [4] and is thus modelled as ζ = ζn0 + w · ζn1. Further is the eigen frequency of the vortex shedding modelled after Brekke's [13] formula :

$$\omega_c = 190 \cdot \frac{133}{100} \cdot \frac{w}{(4.5 + 0.56)} \tag{6}$$

The damping of the shedding ζc is assumed to be a constant. Together this leaves four unknown variables: ζc, a , b , and ζn1 which can be found by fitting the solved equations to the measurements using a least squares method.

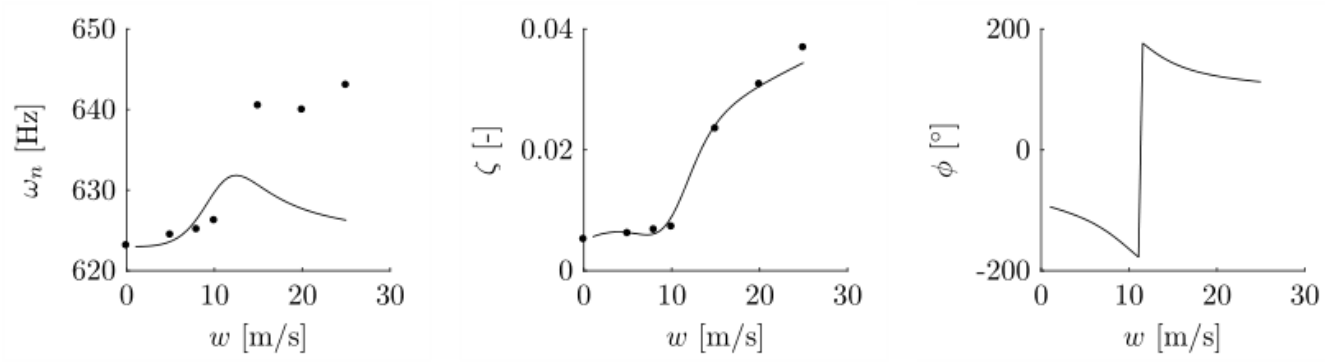

(a) Damping (b) Eigen frequency (c) Phase

Fig. 8 Eigen frequency, Damping and Phase between vortex shedding and foil movement. The dots indicate experimental data, while the line shows the model

Figure 8 shows that the simple model is able to capture the change in damping before and after the lock-in. It does however not capture the entire change in the natural frequency.

3.4 Nonlinear Effects

At this stage, it is appropriate to discuss is whether or not the assumption of linearity that is so often applied in this type of analysis actually holds. A linear system is, by definition, a system which has the following properties: [10]

1. Doubling the magnitude of the excitation force results in a doubling of the response
2. Two or more excitation patterns applied simultaneously results in the sum of the responses, had those forces been applied individually

In order to assess this, future experiments are required. Reese [14] found the experimental setup using a cantilever beam to behave linearly, but only for vibrations in air. There was no test of linearity when the hydrofoil was submerged in water, and exposed to flow.

During our experiment, the frequency response of the foil was found to be somewhat dependent on the excitation amplitude. This is an indicator that the system may not be linear. Two measurements of the frequency response, performed with different excitation amplitudes are shown in Fig. 9.

As Fig. 9 indicates, the FRF is sensitive to variations in excitation amplitude, which could indicate that the system is weakly non-linear. From the FRF, it appears that the damping increases with the excitation amplitude, causing the FRF to peak at a lower amplitude, with a lower natural frequency.

Non-linearities can be unveiled by examination of the inverse frequency response function [10]. For a linear system, the real component of the inverse frequency response function should be linearly proportional to the frequency squared, while the imaginary component of the inverse FRF should be linearly proportional to the frequency. A deviation in this linear relationship to is a strong indicator of a nonlinear system. Such a comparison is shown in Fig. 10.

As shown in Fig. 10, there is some indication that the system may not be strictly linear. It does appear that the non-linearity is more significant at low velocities, where the damping is small, and the vibrational amplitude is large. It is not known how significant the non-linearities are for the measurements, but it is recommended that future measurements investigate whether or not the non-linearities are negligible. In order to investigate this, a constant-response modal analysis is suggested by Ewins, since practically all non-linear behaviour is proportional to response amplitude, and keeping the response amplitude constant should therefore minimize the impact of non-linear behaviour [10].

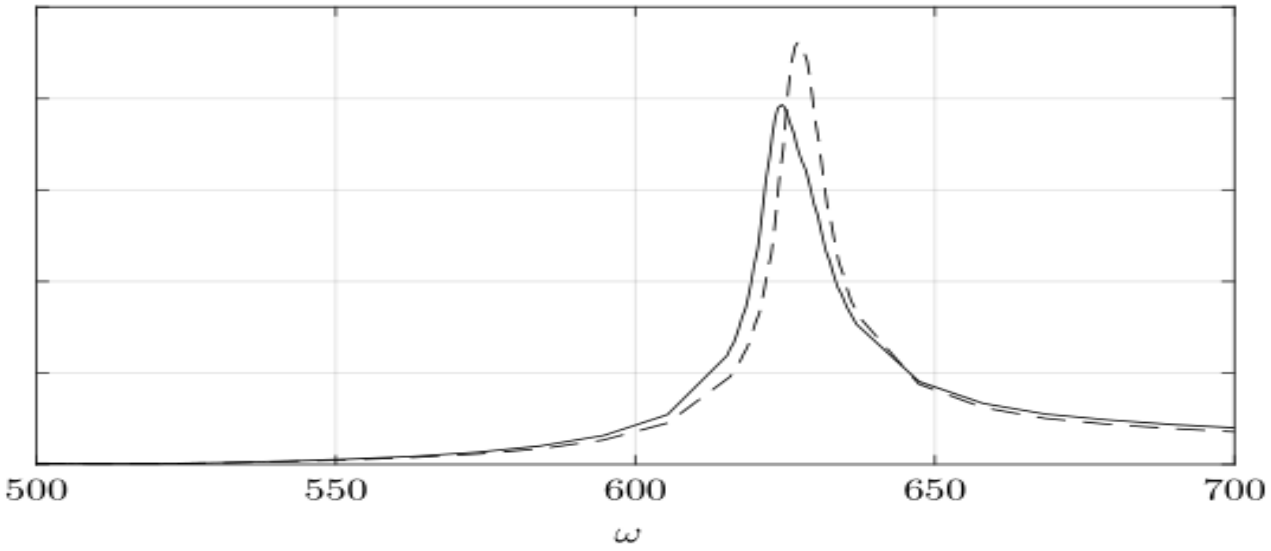

Fig. 9 Frequency response at w = 5 m/s for two different amplitudes of excitation. The dashed line indicates a measurement with a lower excitational amplitude. ω denotes the frequency.

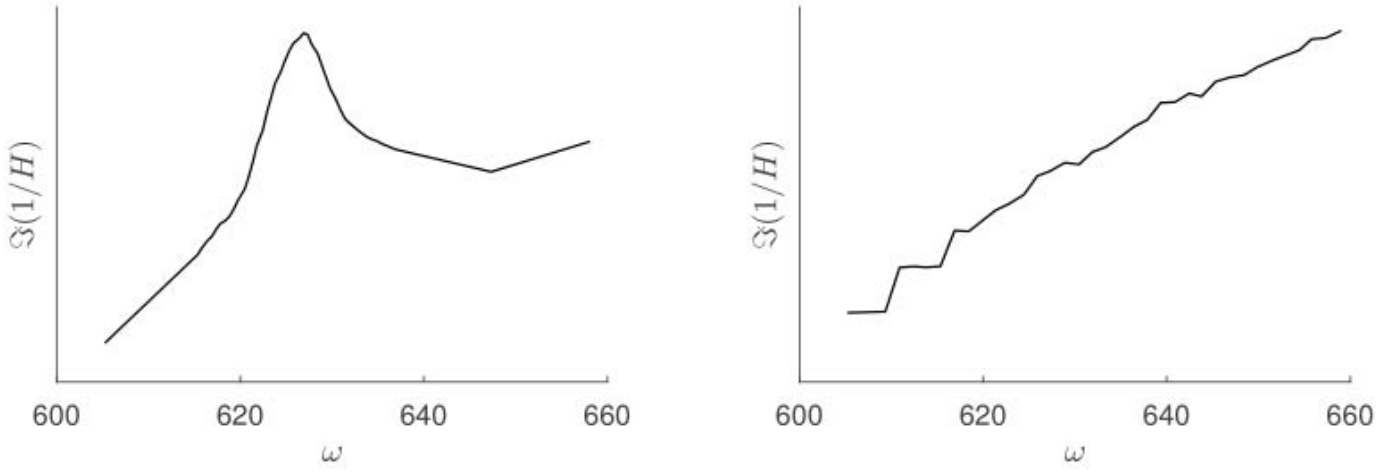

(a) Non-linearity at w =5 m/s

(b) Non-linearity at w =20 m/s

Fig. 10 Imaginary component of the inverse frequency response for the measurement, denoted by 8'(1/H), H being the complex frequency response. Note how the apparent nonlinearity appears to smoothen out as the velocity, and damping, increases.

4. Conclusions

This experiment has shown that there is a linear relationship between the damping ratio and water velocity, thereby confirming previous observations [4, 3, 6]. The natural frequency has been shown to increase linearly for velocities below lock-in, due to the added stiffness of the deflected water. It has also been shown that the dependency on water velocity for both the damping factor and the natural frequency differs for water velocities below and above lock-in, due to the phase shift in vortex shedding when passing through the lock-in region. The damping has been accurately measured through a large number of repetitions for velocities both above and below lock-in. The observed jump in damping and natural frequency when moving through lock in leaves some questions unanswered, such as how the velocity field at the trailing edge changes when moving through lock-in, and how the phase of the pressure on the foil changes with respect to the foil movement. These questions will be further investigated. In addition, there is still some uncertainty in how significant the inherent non-linearity of the experimental setup are, and this will need to be assessed when doing similar experiments in the future.

Nomenclature

a	Mathematical constant	ωn	Natural Frequency of hydrofoil]
b	Mathematical Constant	$\zeta n0$	Damping at zero velocity
ζ	Damping	φ	phase shift
Fy	Deflecting force of a bent beam	$\zeta n1$	Slope of damping increase
x	Trailing edge deflection	ζc	vortex shedding damping
ω	Frequency	ωc	vortex shedding frequency
ωa	Frequency at point a	H	Transfer Function
ωb	Frequency at point b	w	Water velocity
Cl	hydrofoil lift		

References

[1] M. Gagnon and D. Thibault. “Turbine Dynamic Behaviour and Expected Fatigue Reliability,” In: 6th IAHR International Meeting of the Workgroup on Cavitation and Dynamic Problems in Hydraulic Ma- chinery and Systems. Sept. 11, 2015.

[2] M. Flores, G. Urquiza, and J. M. Rodr´ıguez. “A Fatigue Analysis of a Hydraulic Francis Turbine Runner,” In: World Journal of Mechanics 02 (01 2012), pp. 28–34.

[3] A. Coutu et al. “Damping Measurements in Flowing Water,” In: IOP Conference Series: Earth and Environmental Science. Vol. 15. IOP Publishing, 2012, p. 062060.

[4] C. Monette et al. “Hydro-Dynamic Damping Theory in Flowing Water,” In: IOP Conference Series: Earth and Environmental Science. Vol. 22. IOP Publishing, 2014, pp. 32044–32053.

[5] R. R. Craig, A. Kurdila, and R. R. Craig. Fundamentals of Structural Dynamics. 2nd ed. OCLC: ocm61247316. Hoboken, N.J: John Wiley, 2006. 728 pp.

[6] Z. Yao et al. “Effect of Trailing Edge Shape on Hydrodynamic Damping for a Hydrofoil,” In: Journal of Fluids and Structures 51 (Nov. 2014), pp. 189–198.

[7] S. Roth et al. “Hydrodynamic Damping Identification from an Impulse Response of a Vibrating Blade,” In: Proceedings of the 3rd IAHR International Meeting of the Workgroup on Cavitation and Dynamic Problems in Hydraulic Machinery and Systems. Vol. 1. Brno University of Technology, 2009, pp. 253–260.

[8] P. Ausoni et al. “Cavitation Effects on Fluid Structure Interaction in the Case of a 2d Hydrofoil,” In: ASME 2005 Fluids Engineering Division Summer Meeting. American Society of Mechanical Engineers, 2005, pp. 617–622.

[9] O. de la Torre et al. “The Effect of Cavitation on the Natural Frequencies of a Hydrofoil,” In: (Aug. 13, 2012).

[10] D. J. Ewins. Modal Testing: Theory, Practice and Application. 2. ed. Mechanical engineering research studies Engineering dynamics series 10. OCLC: 247979435. Baldock: Research Studies Press, 2000. 562 pp.

[11] C. H. K. Williamson and A. Roshko. “Vortex Formation in the Wake of an Oscillating Cylinder,” In:

[12] Journal of Fluids and Structures 2 (July 1988), pp. 355–381.

[13] R. E. D. Bishop and A. Y. Hassan. “The Lift and Drag Forces on a Circular Cylinder in a Flowing Fluid,” In: Proceedings of the Royal Society of London A: Mathematical, Physical and Engineering Sciences 277.1368 (1964), pp. 32–50.

[14] H. Brekke. “A Review on Oscillatory Problems in Francis Turbine,” In: New Trends in Technologies: Devices, Computer, Communication and Industrial Systems, Sciyo (2010), pp. 217–232.

[15] M. C. Reese. “Vibration and Damping of Hydrofoils in Uniform Flow,” The Pennsylvania State Univer- sity, 2010